A Stranded Unshielded Twisted Pair Modeling for Online Fault Location using OMTDR-based Diagnosis Sensor

Wafa Ben Hassen, Moussa Kafal and Esteban Cabanillas
CEA, LIST, Laboratoire de Fiabilisation et d'Integration des Capteurs Nano-Innov, Bat. 862-PC172, 91191 Gif-sur-Yvette Cedex, France

Keywords: Wiring Diagnosis, Transmission Line Modeling, Stranded Twisted Pair, Reflectometry, OMTDR.

Abstract: Despite the worldwide use of stranded Unshielded Twisted Pair (UTP) cables, scientific references dealing with accurate calculation of distributed parameters of such transmission lines are generally missing, especially in high frequency applications where skin and proximity effects are present. On the other hand, reflectometry is a high frequency method that relies on wave propagation in a cable under test for fault diagnosis. In this context, this paper proposes a distributed parameters model for the lossy transmission line of a stranded UTP cable including the pitch of twist and frequency dependent effects to evaluate as faithfully as possible the reflectometry response in such cables. The developed model is validated with 3D-electromagnetic simulations using Time Domain Reflectometry (TDR). For online diagnosis, Orthognal Multi-Tone Time Domain Reflectometry is performed thanks to its capacity to control bandwidth and enable sensors fusion. In complex wiring networks, the developed model is performed to evaluate the performance of OMTDR-based diagnosis sensor including a Xilinx Zynq 7010 FPGA, 10-bit Analog-to-Digital Converter (ADC) and Digital-to-Analog Converter (DAC).

1 INTRODUCTION

Electrical wiring are usually implemented in environments sensitive to severe conditions (aeronautics, naval, space, etc.) thus exposing cables to dangerous situations and problems (Auzanneau, 2013). For instance, cutting a wire in a cable can cause the loss of functionality of one or more critical systems. Thus, the need for a system to online diagnose faults in the electrical wiring in an alive mode becomes essential to facilitate maintenance, minimize downtime, etc. Orthogonal Multi-Tone Time Domain Reflectometry (OMTDR) has the advantage of being simple to analyze: the impedance faults or discontinuities present on the cable are represented by peaks on the corresponding reflectogram (Hassen et al., 2013). For a Maintenance Repair Overhaul (MRO) application, the diagnosis sensor is connected to the cable giving access to the network in which a fault has been identified in an effort to characterize the fault (detection, localization and identification) (Kafal et al., 2018). However, a reflectogram could be very complex to analyze due to the measurement noise, the network complexity, the phenomenon of attenuation, etc.

In fact, the presence of Impedance Discontinuities (IDs) along the cable may locally disturb the propagation of the test signal, subsequently provide undesirable signals and thus increase the noise level of the reflectometry measurement. The diagnosis performance may be limited by the resistance of the cable leading to signal attenuation. This phenomenon is mainly encountered on long cables, and becomes more important in the presence of connectors for connecting the different sections of the cable networks. In the presence of one or sometimes all of the above constraints, the reflectogram acquired by the diagnosis system can be very complex to analyze and interpret. However, it is essential to provide clear and precise information regarding the fault to technicians responsible for accurately performing cables maintenance and repair. For this reason, modeling and simulating transmission lines is necessary to evaluate the reflectometry response according to the test signal frequency, cable length, network topology, coupling, etc.

Within this context, the current paper proposes a distributed parameter model for a lossy transmission line of a stranded Unshielded Twisted Pair (UTP) cable. In fact, state of the art shows that most scientific references consider twisted pairs as parallel wires and replace air with uniform dielectric without considering the effect of twists on the characteristic impedance, coupling, and so on (Truong, 2000).

Ben Hassen, W., Kafal, M. and Cabanillas, E.
A Stranded Unshielded Twisted Pair Modeling for Online Fault Location using OMTDR-based Diagnosis Sensor.
DOI: 10.5220/0007387000400046
In *Proceedings of the 8th International Conference on Sensor Networks (SENSORNETS 2019)*, pages 40-46
ISBN: 978-989-758-355-1

Moreover, stranded cables are generally considered as a solid core. These assumptions are unsuitable, particularly, at high frequencies since stranded cables have larger resistances compared to solid core ones (Meng et al., 2002). To counter these effects, we developed in this paper a model that takes into account the pitch of twist, strand area per conductor and frequency dependent effects (i.e. skin effect, proximity effect, etc.). The developed model is validated with 3D-electromagnetic simulations using Time Domain Reflectometry (TDR). To ensure online diagnosis, Orthogonal Multi-Tone Time Domain Reflectometry is used thanks to its capacity to control bandwidth and enable sensors fusion (Cabanillas et al., 2018b; Hassen et al., 2018). In complex wiring networks, the developed model is used to evaluate the performance of the OMTDR-based diagnosis sensor including Xilinx Zynq 7010 FPGA, 10-bit Analog-to-Digital Converter (ADC) and Digital-to-Analog Converter (DAC) in different configurations (Cabanillas et al., 2018a).

The rest of the paper is organized as follows: In section 2, the distributed parameters model of a twisted pair is introduced. The validation of the developed model is verified by 3D electromagnetic simulations in section 3. After that, section 4 proposes to study the behavior of the developed model of the twisted pair as a function of the signal frequency, pitch of twist, and cable length. In section 5, an evaluation of the OMTDR-based sensor in complex wiring networks is performed.

2 TRANSMISSION LINE MODEL

An UTP is a transmission line composed of two conductors spirally wound around each other to limit sensitivity to interference and cross-talk. It is widely used in the aeronautical field for controller application not limited to the Controller Area Network (CAN) bus, MIL-STD-1553B, etc. The characteristic impedance, Z_c, of a transmission line is a function of the distributed parameters (per unit length) series Resistance R, series inductance L, shunt capacitance C, and shunt conductance G. The characteristic impedance is thus defined as follows:

$$Z_c = \sqrt{\frac{R + j2\pi fL}{G + j2\pi fC}}. \tag{1}$$

where f is the frequency. In the case of a lossy twisted-pair transmission line, distributed parameters are modeled using electrical and geometrical properties such as conductor diameter, dielectric loss, etc. The helical pitch angle of twist influences the dielectric constant denoted ε_{eq} and is calculated in equation (2) as follows (Lefferson, 1971):

$$\theta = \tan^{-1}(2T\pi D), \tag{2}$$

where T is the number of twists per meter and D is the distance between the centers of conductors. The twist correction factor is then used to adjust the dielectric constant in equation (3) as follows (Truong, 2000):

$$q = 0.45 + 10^{-3}\left(\theta \cdot \frac{180}{\pi}\right)^2. \tag{3}$$

The equivalent dielectric constant integrating the influence of the twist angle ε_{eq} can be calculated in equation (4) as follows (Kasthala and Venkatesan, 2016):

$$\varepsilon_{eq} = 1 + q\,(\varepsilon_r - 1)\,, \tag{4}$$

where ε_r is the relative permittivity. With the determined equivalent dielectric constant, the capacity can be described as:

$$C = \frac{\pi\varepsilon_0\varepsilon_{eq}}{\log_{10}\left(\frac{D}{d} + \sqrt{\left(\frac{D}{d}\right)^2 - 1}\right)}, \tag{5}$$

where, the parameter ε_0 is the permittivity of air. In the same manner, the inductance per unit length of the cable is given in (6):

$$L = \frac{\mu_0\mu_r}{\pi}\log_{10}\left(\frac{D}{d} + \sqrt{\left(\frac{D}{d}\right)^2 - 1}\right), \tag{6}$$

where μ_0 is the permeability of free space and μ_r is the relative permeability of the dielectric.

Since reflectometry operates at a high frequency to ensure accurate fault location, the model must reflect the behavior of the transmission line at such bands. In this context, there are two factors that determine the current distribution on the conductor cross-section. The first is the *skin effect* which, for high frequency, causes a concentration of the current near the outer surfaces of the cylindrical conductor (Wheeler, 1942). When a current flows through two or more adjacent conductors, the current distribution in a conductor is affected by the magnetic flux produced by the adjacent conductors, as well as by the magnetic flux produced by the current in the conductor itself. This phenomenon is called *proximity effect* and causes a resistance value greater than that of a simple skin effect (Ferkal et al., 1996). In this paper, we note the proximity factor P that is determined according to the ratio between D and d as described in (Smith, 1971).

For a twisted pair with n strands per conductor, one can calculate the resistance per unit-length in (7), where d_s is the strand diameter:

$$R(f) = P\left(\frac{2n}{\pi d \delta \sigma}\right)\left(\frac{d_s}{d}\right)^2, \quad (7)$$

where the skin effect δ is expressed in (8) as follows:

$$\delta = \frac{1}{\sqrt{\pi \mu \sigma f}}, \quad (8)$$

where $\mu = \mu_0 \mu_r$ being the dielectric permeability, σ the conductor conductivity and f the frequency. The conductance per unit length G is given in (9) as:

$$G(f) = 2\pi f C \tan\delta, \quad (9)$$

where $\tan\delta$ is the tangent of the dielectric loss and depends on the frequency.

The behavior of the characteristic impedance of a lossless UTP according to twist pitch is studied later in the current paper. For this reason, the twist correction factor $q(\xi)$ may be expressed as a function of the twist pitch as follows (Truong, 2000):

$$q(\xi) = 0.45 + 10^{-3}\xi^2. \quad (10)$$

where ξ is the twist pitch. In the case of a lossless UTP cable where $D \simeq d$, the characteristic impedance may be expressed in function of the twist pitch as:

$$Z_c(\xi) = \sqrt{\frac{L}{C}} = \frac{1}{\pi}\log\left(\frac{D}{d}\right)\sqrt{\frac{\mu}{\varepsilon_0 \varepsilon_{eq}(\xi)}}. \quad (11)$$

where $\varepsilon_{eq}(\xi)$ is the equivalent permittivity constant and is computed according to (4) using $q(\xi)$ formula (10) rather than q formula (3).

3 RLCG MODEL VALIDATION

In this section, we propose to validate the distributed parameters model described in section (2). For this, the distance between the two conductors is $D = 0.95$ *mm* and the diameter of a conductor is $d = 0.75$ *mm*. The strands are made of copper ($\sigma = 5.810^7$ S/m) and the insulation is made of Teflon ($\varepsilon_r = 2.1$ and $\mu = 4\pi 10^{-7}$) . The proximity factor $P = 2.1$ is determined directly from the curve provided in (Smith, 1971) for a ratio $\left(\frac{D}{d}\right) = 1.2$. To reconstruct the reflectogram from the secondary parameters calculated on the basis of R, L, C and G, the transfer function expressed as follows can be used:

$$H(f) = \Gamma_E + \frac{(1-\Gamma_E^2)\Gamma_L e^{-2\gamma l}}{1+\Gamma_E \Gamma_L e^{-2\gamma l}}, \quad (12)$$

where l is the length of the cable, Γ_E and Γ_L are, respectively, the reflection coefficients at the input and output of the line and γ is the propagation constant. The propagation constant γ is given by:

$$\gamma = \sqrt{(R + j2\pi fL)(G + j2\pi fC)}. \quad (13)$$

The reflection coefficient Γ_E at the input of the line is calculated as follows:

$$\Gamma_E = \frac{Z_c - Z_0}{Z_0 + Z_c}. \quad (14)$$

with Z_0 is the impedance of the generator. In this case, it is considered equal to 50Ω. In the case of an open circuit at the end of the line, the reflection coefficient is defined $\Gamma_L = 1$.

In order to validate the distributed parameters model, a 3D electromagnetic (EM) model of an UTP is developed using a dedicated 3D-electromagnetic simulation software as shown in figure 1. The model consists of 19 copper strands per conductor. The diameter of one strand is 0.15 *mm*. The diameter of the conductor is 0.75 *mm*. The conductor is covered by a thin layer of Teflon insulation whose thickness is 0.08 *mm*. The distance between the two conductors is 0.95 *mm* and the number of twist steps is 100 per meter. The length of the model is 1 *m*. A local mesh is performed, as shown in figure 2, with a step width in absolute value as follows: $x = 0.1$ *mm*, $y = 0.04$ *mm* and $z = 0.04$ *mm*. The total number of meshes is 37 004 352. The 19 strands per conductor are connected to a central point through 19 lines with perfect conductivity and lengths of 0.5 *mm*. The port with a 50 Ω impedance connects the two conductors through the center points as shown in figure 3 to inject/receive test signals.

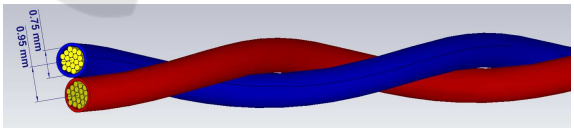

Figure 1: The developed 3D EM model of a stranded USTP.

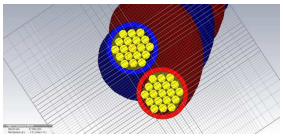

Figure 2: The 3D model mesh.

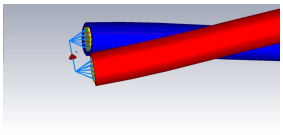

Figure 3: The 3D model port.

Figure 4 shows the TDR reflectograms of the RLCG-based model and the 3D EM model. For these simulations, the used bandwidth is ranged from 0 *Hz* to 1 *GHz* and the width of the Gaussian pulse, used as test signal, is 1 *ns*.

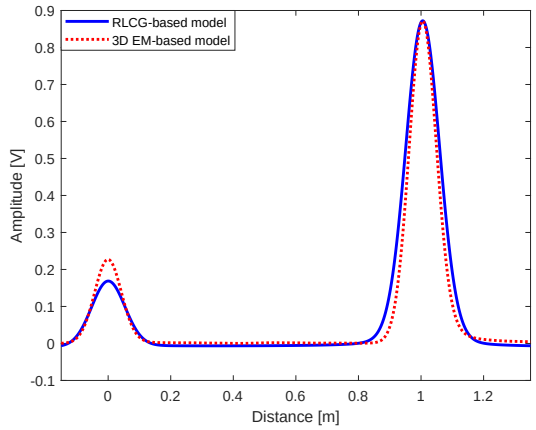

Figure 4: TDR reflectograms of the RLCG-based model and 3D EM model.

The correlation coefficient is used to compare the similarity between the data from the calculated distributed parameters model and that of the 3D electromagnetic simulations. Here, it is considered that the data is strongly correlated if the correlation coefficient is between 0.9 and 1. In this context, the correlation coefficient between the two reflectograms resulting from the calculated RLCG model and the 3D model is equal to 0.9855. One can thus consider that the correlation coefficient is strong and one can validate the model with distributed constants developed in section (2) in the case of a twisted pair. The amplitude of the peak of the open circuit present at the end of the cable is equal to 0.86 V knowing that the amplitude of the Gaussian pulse is $1V$. It is important to note that the correlation coefficient between the two reflectograms resulting directly from the model proposed in (Truong, 2000) and the 3D model is equal to 0.2222. After RLCG-based model validation, the following section proposes to study the UTP behavior.

4 UTP PARAMETERS ANALYSIS

The RLCG parameters may be calculated based on physical and electrical proprieties of the transmission line such as conductor diameter, material, stranding, etc. On the other hand, these parameters may also be estimated based on the channel response measurement (Cohen and Gregis, 2014; Jiao and Liao, 2017) when the exact properties of the transmission line are not available on the cable data sheet. Here, the RLCG parameters are calculated in the following order starting with equation (7), (6), (5) and ending with (9). They may be also estimated according to (Cohen and Gregis, 2014) where the length of the transmission line is 1 m, the width of the Gaussian pulse is $1ns$ and finally the obtained reflectogram of the 3D-based model shown in figure 4 (red curve) are used as inputs of the considered algorithm.

Figure 5 presents the increase of the resistance R and of the conductance G as a function of frequency, respectively. It shows also that the capacitance (C) and inductance (L) do not depend on frequency.

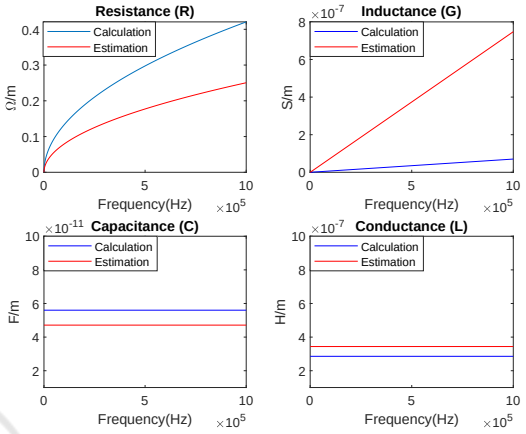

Figure 5: Variation of calculated and estimated RLCG parameters of the twisted pair as a function of the frequency.

The phase angle $\Phi(f)$ of the characteristic impedance of $Z_c(f)$ is given by:

$$\Phi(f) = \text{angle}\left(\text{Re}(Z_c(f)), \text{Im}(Z_c(f))\right)\frac{180}{\pi}. \quad (15)$$

Figure 6 (top) demonstrates the modulus of the characteristic impedance as a function of the frequency whereas figure 6 (bottom) shows the phase of the characteristic impedance as a function of the frequency. The characteristic impedance is 71.4Ω in this case study.

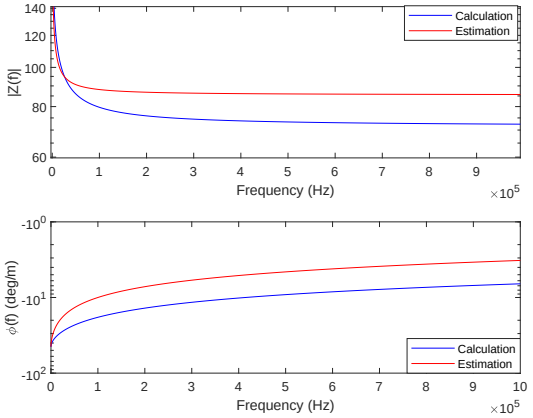

Figure 6: Variation of the characteristic impedance Z_c as a function of the frequency.

The attenuation of the cable in dB/m is given as follows:

$$\alpha(f) = \frac{-20}{\log(10)}\mathrm{Re}(\gamma(f)). \quad (16)$$

The phase constant in $degree/m$ is given as:

$$\beta(f) = \frac{180}{\pi}\mathrm{Im}(\gamma(f)). \quad (17)$$

Figure 7 (top) and figure 7 (bottom) show the increase of the attenuation according to (16) and of the phase constant according to (17) as a function of frequency, respectively.

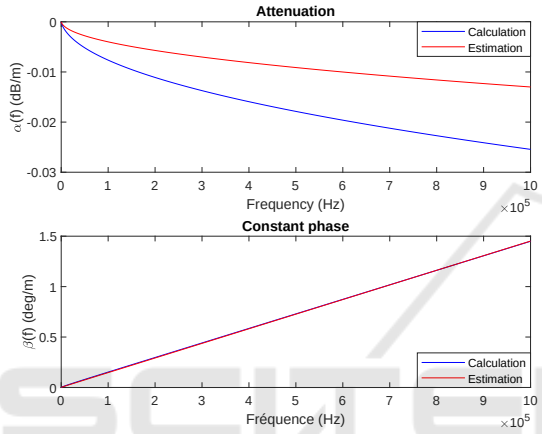

Figure 7: Attenuation and phase constant versus frequency.

It is noteworthy that the frequency of the reflectometry signal is a critical parameter in detecting and locating a fault in a cable. Indeed, the higher the frequency of the reflectometry signal, the better is the resolution of the reflectogram and the localization accuracy of small defects. However, in the case of fault detection on long cables, increasing the signal frequency is not recommended as it introduces dispersion and increase in signal attenuation. TDR simulations were performed on the RLCG model for a length of 100 m. In this context, the peak amplitude of the open circuit is 0.0084 V and 0.065 V for a frequency of 2 GHz and 200 MHz, respectively.

Figure 8 demonstrates the variation of the characteristic impedance as a function of the twist pitch in a lossless UTP cable. It can be noted that the characteristic impedance decreases with the increase of the twist pitch. Indeed, the variation of twist pitch throughout the cable can significantly affect the characteristic impedance of the twisted pair and thus introduce multiple reflections on the reflectogram.

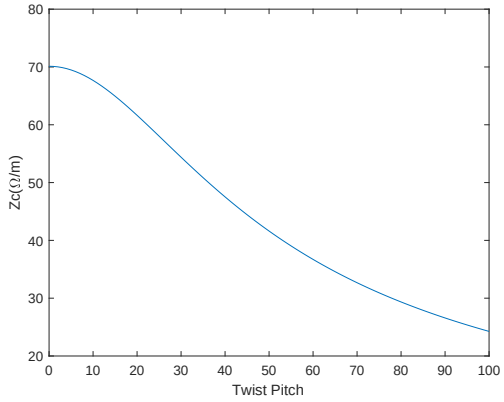

Figure 8: The characteristic impedance Z_c according to the twist step ξ.

5 EXPERIMENTAL RESULTS

The development of the distributed parameter model permits to evaluate the reflectometry response in different configurations and hence avoid the development of test benches leading to a gain in cost and time. For experimental validations, a 10 m long UTP EN 2267-009 DRB 24 cable is connected to an electronic board that permits to inject/receive OMTDR signals. The electronic board includes FPGA SoC Xilinx ZyNQ 7010, 10-bits ADC, 10-bits DAC and 512 Megabyte DDR chip as shown in figure 9.

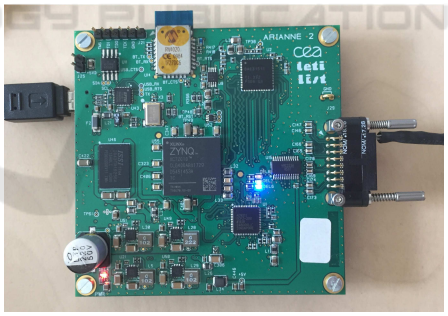

Figure 9: The electronic board used for generating, injecting and receiving the OMTDR signals into a tested wiring network.

An OMTDR based signal composed of 128 subcarriers over a total bandwidth ranging from 300 KHz to 1.5 GHz with 2048 frequency samples has been generated and injected into the tested network. The principle of OMTDR is shown in figure 10.

For numerical results, the processing performed by the electronic board is modeled using Matlab simulations (i.e, analog to digital conversion, digital to analog conversion, oversampling, measurement noise, etc.). Figure 11 shows the OMTDR based-reflectogram of the UTP model and the measured one

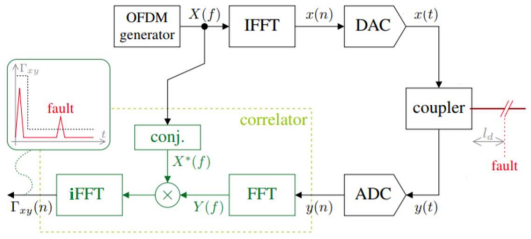

Figure 10: Schematic diagram of an OMTDR reflectometry.

on a 10 *m* cable. The open circuit present at the end of the cable is represented in the reflectogram by an amplitude peak 0.36 with respect to the amplitude of the peak at the input of the reflectogram. In the same configuration, the open circuit present at the end of the cable with 100 *m*-length is represented by a peak of amplitude 0.03 with respect to the amplitude of the peak at the input of the transmission line.

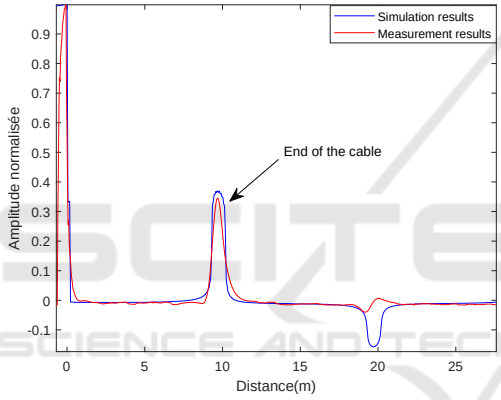

Figure 11: OMTDR reflectograms of the RLCG model of the twisted pair 30 m long.

For complex networks, a double Y-junction network topology was implemented using UTP EN 2267-009 DRB 24 cables as depicted in figure 12. The extremities of the network were left open and one extremity served as a testing port. The tested network consists in 5 branches and 2 junctions.

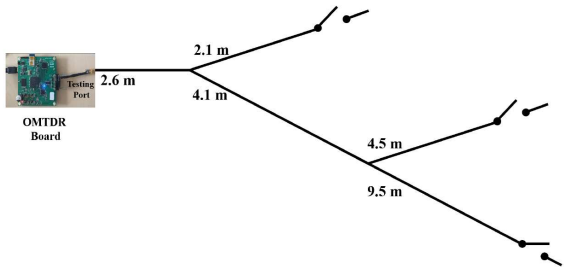

Figure 12: Layout of the double Y-junction NUT considered for the experimental validation of the developed model.

Figure 13 shows the OMTDR reflectometry response of the UTP cable model in complex networks as the double Y-junction configuration of figure 12.

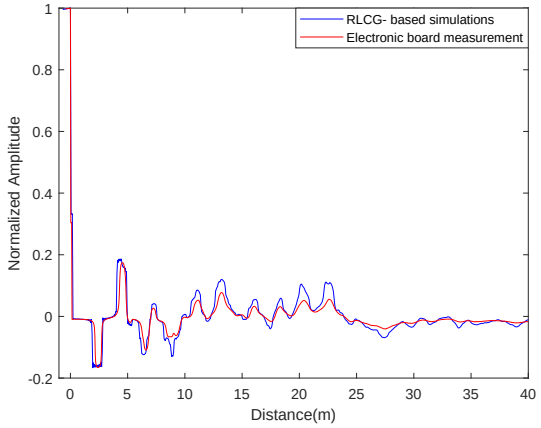

Figure 13: The measured and simulation OMTDR responses of the tested NUT

The distributed-constant model of the twisted pair may be extended to other twisted pairs. It suffices to define the geometrical properties (for example, conductor radius, distance between two conductors, etc.) and the electrical properties (for example, permittivity, conductivity, etc.) to determine the primary and subsequently secondary parameters. It is then sufficient to define the topology of the cable network to evaluate the performance of the on-board diagnostic system in the desired configuration (connector, splice, etc.).

6 CONCLUSION

In this paper, a distributed parameters model of a stranded twisted pair has been introduced. This model has been validated by 3D electromagnetic simulations of an unshielded twisted pair cable. The developed model could be extended to other twisted pairs subject to knowing their geometric and electrical properties. This model permits to evaluate the diagnosis system (i.e. electronic board, etc.), in the desired configuration of a twisted pair without resorting to the establishment of a test bench.

REFERENCES

Auzanneau, F. (2013). Wire troubleshooting and diagnosis: Review and perspectives. *Progress In Electromagnetics Research*, 49:253–279.

Cabanillas, E., Kafal, M., and Ben-Hassen, W. (2018a). On the implementation of embedded communication over

reflectometry-oriented hardware for distributed diagnosis in complex wiring networks. In *2018 IEEE AUTOTESTCON*, pages 1–6. IEEE.

Cabanillas, E., Layer, C., Kafal, M., and Dupret, A. (2018b). Enhancing the spatial resolution for wire fault detection systems using multi-carrier signals. *IEEE Sensors Journal*, 18(23):9857–9866.

Cohen, J. and Gregis, N. (2014). Method of determining lineal parameters of a transmission line.

Ferkal, K., Poloujadoff, M., and al (1996). Proximity effect and eddy current losses in insulated cables. *IEEE transactions on Power Delivery*, 11(3):1171–1178.

Hassen, W. B., Auzanneau, F., Incarbone, L., Pérès, F., and Tchangani, A. P. (2013). Omtdr using ber estimation for ambiguities cancellation in ramified networks diagnosis. In *Intelligent Sensors, Sensor Networks and Information Processing, 2013 IEEE Eighth International Conference on*, pages 414–419. IEEE.

Hassen, W. B., Kafal, M., Cabanillas, E., and Benoit, J. (2018). Power cable network topology reconstruction using multi-carrier reflectometry for fault detection and location in live smart grids. In *2018 Condition Monitoring and Diagnosis (CMD)*, pages 1–5. IEEE.

Jiao, X. and Liao, Y. (2017). A linear estimator for transmission line parameters based on distributed parameter line model. In *Power and Energy Conference at Illinois (PECI), 2017 IEEE*, pages 1–8. IEEE.

Kafal, M., Mustapha, F., Hassen, W. B., and Benoit, J. (2018). A non destructive reflectometry based method for the location and characterization of incipient faults in complex unknown wire networks. In *2018 IEEE AUTOTESTCON*, pages 1–8. IEEE.

Kasthala, S. and Venkatesan, G. P. (2016). Experimental verification of distributed parameters on indian residential networks for power line communication. *Internatioanl Journal of Engineering and Technology*, 8(6):2845–2852.

Lefferson, P. (1971). Twisted magnet wire transmission line. *IEEE Transactions on Parts, Hybrids, and Packaging*, 7(4):148–154.

Meng, H., Chen, S., and al (2002). A transmission line model for high-frequency power line communication channel. In *International Conference on Power System Technology*, volume 2, pages 1290–1295.

Smith, G. (1971). The proximity effect in systems of parallel conductors and electrically small multiturn loop antennas. Technical report, Harvard Univ Cambridge Ma Div Of Engineering And Applied Physics.

Truong, T. K. (2000). Twisted-pair transmission-line distributed parameters. *EDN Mag.*

Wheeler, H. A. (1942). Formulas for the skin effect. *Proceedings of the IRE*, 30(9):412–424.